

Supporting Information

Multiphoton Light Emission in Barium Stannate Perovskite Driven by Oxygen Vacancy, Eu³⁺ and La³⁺: Accessing the Role of Defect and Local Structure

Santosh K. Gupta^{1,5*}, B. Modak^{2,5}, Debarati Das,¹ P. Modak^{3,5}, A.K. Yadav,⁴ K. Sudarshan^{1,5*}

¹Radiochemistry Division, Bhabha Atomic Research Centre, Trombay, Mumbai-400085, India

²Chemistry Division, Bhabha Atomic Research Centre, Trombay, Mumbai-400085, India

³Radiological Safety Division, Atomic Energy Regulatory Board, Anushaktinagar, Mumbai – 400094, India

⁴Atomic and Molecular Physics Division, Bhabha Atomic Research Centre, Trombay, Mumbai-400085, India

⁵Homi Bhabha National Institute, Anushaktinagar, Mumbai – 400094, India

*To whom correspondence should be addressed. Electronic mail: santoshg@barc.gov.in, santufrnd@gmail.com (SKG), kathis@barc.gov.in (KS)

S1. Sample preparation

The samples were prepared by solid state method. For preparation of BaSnO₃; BaCO₃ and SnO₂ in 1:1 molar ratio were well grounded and annealed at 900 °C for 5 hours, cooled to room temperature in air, grounded and annealed further at 1200 °C for 5 hours. The heating rate was 10deg. per minute. The samples were powdered again and used in all the measurements. For Eu doping, 0.5 mole % of Eu₂O₃ with respect BaCO₃ (1 mol% Eu with respect Ba) was mixed along with the BaCO₃ and SnO₂ and grounded before annealing. In La codoped samples, the requisite mole % of La₂O₃ was added in addition to Eu₂O₃.

S2 Instrumentation

Powder X-ray diffraction measurements were carried out using a table top AXRD instrument (Proto Make) in the 2θ range of 20 to 70deg and Cu Kα (λ=1.5405 Å) as monochromatic x-ray source. The scan rate was 2 deg per minute. Reitveld analysis of the samples was carried out using the program FULLPROF.¹Initial estimates of the lattice parameters were taken from ICSD: 190601.²

An Edinburgh make florescence spectrometer (model CD 920) was used for the photoluminescence measurements. Xenon flash lamp (μF2) and power-150 Watt was used as the excitation source. Both the emission and excitation spectra were recorded with a step of 1.0 nm per second at lamp frequency of 100 Hz while emission lifetimes were measured with chosen excitation and emission wavelengths using time-correlated single-photon counting (TCSPC) technique at lamp frequency of 10 Hz.

Positron annihilation lifetime measurements were carried out using a lifetime spectrometer set up using a barium fluoride detector and a lanthanum bromide detector. The spectrometer has a time resolution 265 ps. 15 μCi Carrier free ^{22}Na deposited between two 8 micron polyimide films was the source of positrons and it was immersed in the powder so that all positrons annihilate in the sample. All the lifetime spectra were acquired for a million counts and were analyzed using PALSFit³ after correcting for the positrons annihilating in the polyimide films used to deposit ^{22}Na . SEM images were recorded on a SNE4500 Mini SEM instrument.

S3. Theoretical methodology

We have performed density functional theory (DFT) based first-principles calculations using Vienna ab-initio simulation package (VASP).^{4,5} The projector augmented wave (PAW) pseudo potentials were used for the ion-electron interactions including the valence states of Ba ($5s^25p^66s^2=$ 10 valence electrons), Sn ($5s^25p^2,$ = 4 valence electrons), Eu ($5p^66s^25d^1=$ 9 valence electrons), La ($5s^25p^66s^25d^14f^0=$ 11 valence electrons) and O ($2s^22p^4 =$ 4 valence electrons). However, during electronic structure calculation we have chosen potential considering 17 valence electrons for Eu ($5s^25p^66s^25d^04f^7$). The generalized gradient approximations (GGA) of Perdew–Burke–Ernzerhof (PBE) were used during the structure optimization procedure.^{6,7} The plane wave basis with kinetic energy cut off of 550 eV and energy convergence of 10^{-6} eV for self-consistent iteration have been chosen. Brillouin zone sampling has been performed by Γ -centered k-point mesh of $8 \times 8 \times 8$ using Monkhorst and Pack scheme.⁸ For all the model structures, the relaxation of both cell parameter and ionic positions during geometry optimization has been taken into account. The optimized geometries are used to calculate the electronic structure of the system using PBE0 hybrid density functional. According to PBE0 functional, exchange functional is treated with both PBE exchange (E_X^{PBE}) and exact Hatree-Fock (HF) exchange (E_X), while the correlation part is completely defined by PBE functional (E_C^{PBE}).^{9,10} Thus, the exchange-correlation energy (E_{XC}^{PBE0}) can be expressed as,

$$E_{XC}^{PBE0} = \frac{1}{4}E_X + \frac{3}{4}E_X^{PBE} + E_C^{PBE} \quad (1)$$

For the calculation of density of states (DOS) we have chosen tetrahedron method with Blöchl correction.¹¹

S4. Positron lifetimes

The positron lifetimes for saturation trapping of positrons in various kinds of defects envisaged in BaSnO₃ and in the defect free system were calculated using the MIKA Doppler program.¹² The lattice parameters and coordinates of the atoms in BaSnO₃ were taken from reported literature and used.¹³ Possible relaxation of ions around the vacancies and changes in the coordinates of the ions due to aliovalent substitutions in the lattice were not considered in determining the lattice positions. A 4x4x4 super cell was considered for the calculations and the atomic superposition of free atoms was considered to determine the electron density of the solid. Electron-positron correlations were taken within the generalized gradient approximation.¹⁴ The enhancement factors were taken as given by Arponen–Pajanne–Barbiellini approximation.¹⁵

S5. Synchrotron EXAFS and XANES Measurements

An X-ray Absorption Spectroscopy (XAS) measurement, which comprises of both X-ray Near Edge Structure (XANES) and Extended X-ray Absorption Fine Structure (EXAFS) techniques, have been carried out on BaSnO₃ and Eu doped BaSnO₃ at Sn K edge and Eu L₃ edge to probe the local structure. The XAS measurements have been carried out at the Energy-Scanning EXAFS beamline (BL-9) at the Indus-2 Synchrotron Source (2.5 GeV, 100 mA) at Raja Ramanna Centre for Advanced Technology (RRCAT), Indore, India.^{16,17} This beamline operates in the energy range of 4 KeV to 35 KeV. The beamline optics consists of a Rh/Pt coated collimating meridional cylindrical mirror and the collimated beam reflected by the mirror is monochromatized by a Si(111) ($d=6.2709 \text{ \AA}$) based double crystal monochromator (DCM). The second crystal of DCM is a sagittal cylinder used for horizontal focusing while a Rh/Pt coated bendable post mirror facing down is used for vertical focusing of the beam at the sample position. Rejection of the higher harmonics content in the X-ray beam is performed by detuning the second crystal of DCM. The edge jump (ΔE) of 1.18 and 1.06 are obtained at Sn K-edge using the optimized weight of the sample pallet of BaSnO₃ and Eu doped BaSnO₃, respectively. The Fourier transform range of 3-10 \AA^{-1} with Hanning window is used for both the edges and the R range of 1-4.5 \AA and 1-3 \AA are used for back transform and fitting purpose at Sn K-edge and Eu L₃-edge, respectively.

In the present case, XAS measurements have been performed in transmission mode at Sn K-edge and fluorescence mode at Eu L₃-edge.

For the transmission measurement, three ionization chambers (300 mm length each) have been used for data collection, one ionization chamber for measuring incident flux (I_0), second one for measuring transmitted flux (I_t) and the third ionization chamber for measuring XAS spectrum of a reference metal foil for energy calibration. Appropriate gas pressure and gas mixtures have been chosen to achieve 10-20% absorption in first ionization chamber and 70-90% absorption in second ionization chamber to improve the signal to noise ratio. The absorption coefficient μ is obtained using the relation:

$$I_T = I_0 e^{-\mu x} \quad (1)$$

where, x is the thickness of the absorber. In case of fluorescence mode, silicon drift detector is used to measure the fluorescence intensity I_f and ionization chamber for measuring incident flux (I_0). The absorption coefficient is obtained using the relation $\mu = I_f/I_0$.

The local structure around the absorbing atom is obtained from the quantitative analysis of EXAFS spectra. In order to take care of the oscillations in the absorption spectra $\mu(E)$ has been converted to absorption function $\chi(E)$ defined as follows:¹⁸

$$\chi(E) = \frac{\mu(E) - \mu_0(E)}{\Delta\mu_0(E_0)} \quad (2)$$

where, E_0 is absorption edge energy, $\mu_0(E_0)$ is the bare atom background and $\Delta\mu_0(E_0)$ is the step in $\mu(E)$ value at the absorption edge. The energy dependent absorption coefficient $\chi(E)$ has been converted to the wave number dependent absorption coefficient $\chi(k)$ using the relation,

$$K = \sqrt{\frac{2m(E - E_0)}{h^2}} \quad (3)$$

where, m is the electron mass. $\chi(k)$ is weighted by k^2 to amplify the oscillation at high k and the $\chi(k)k^2$ functions are Fourier transformed to generate the $\chi(R)$ versus R plots in terms of the real distances from the center of the absorbing atom. The set of EXAFS data analysis programme available within Demeter software package have been used for EXAFS data analysis.¹⁹ This includes background reduction and Fourier transform to derive the $\chi(R)$ versus R plots from the absorption spectra (using ATHENA software), generation of the

theoretical EXAFS spectra starting from an assumed crystallographic structure and finally fitting of experimental data with the theoretical spectra using ARTEMIS software.

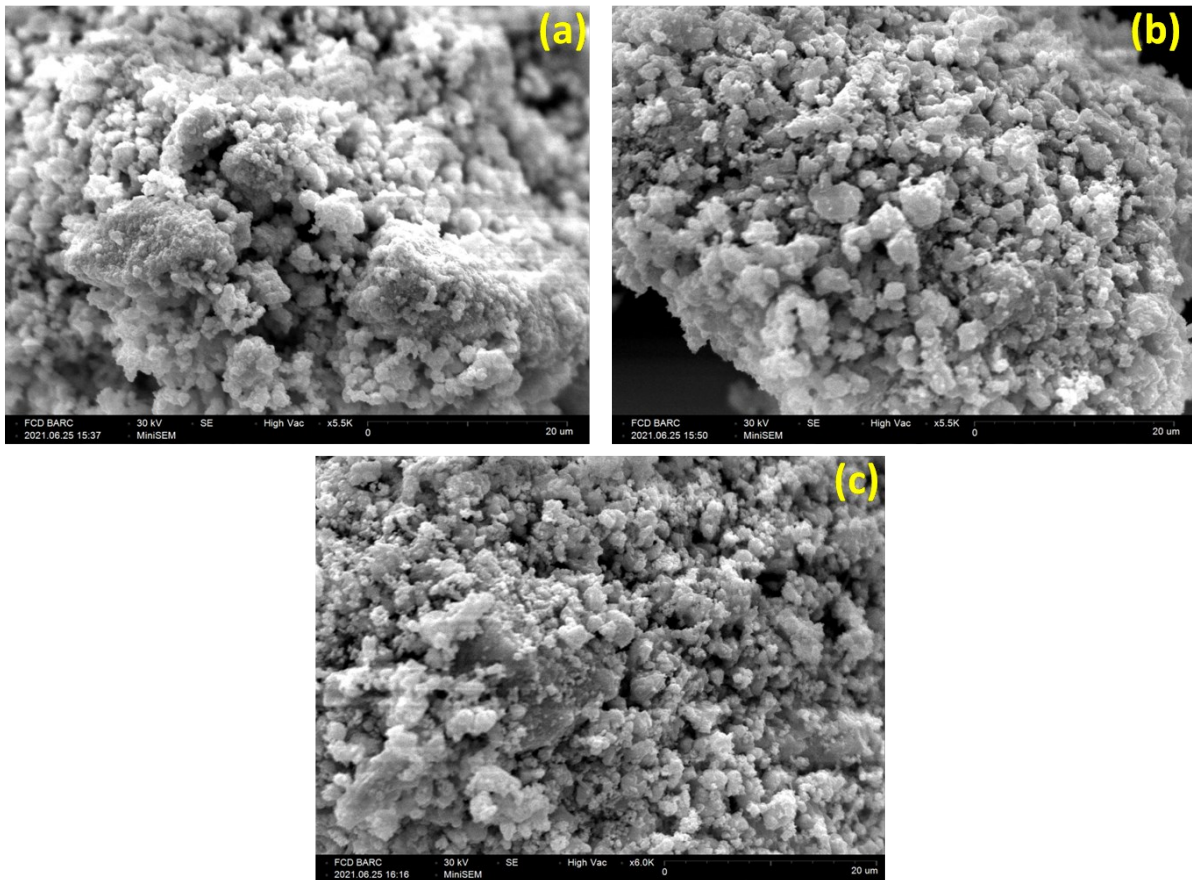


Figure S1: SEM images of (i) Undoped (ii) 1.0 % Eu³⁺ doped and (iii) 1.0 % Eu³⁺, 5.0 % La³⁺ co-doped BaSnO₃

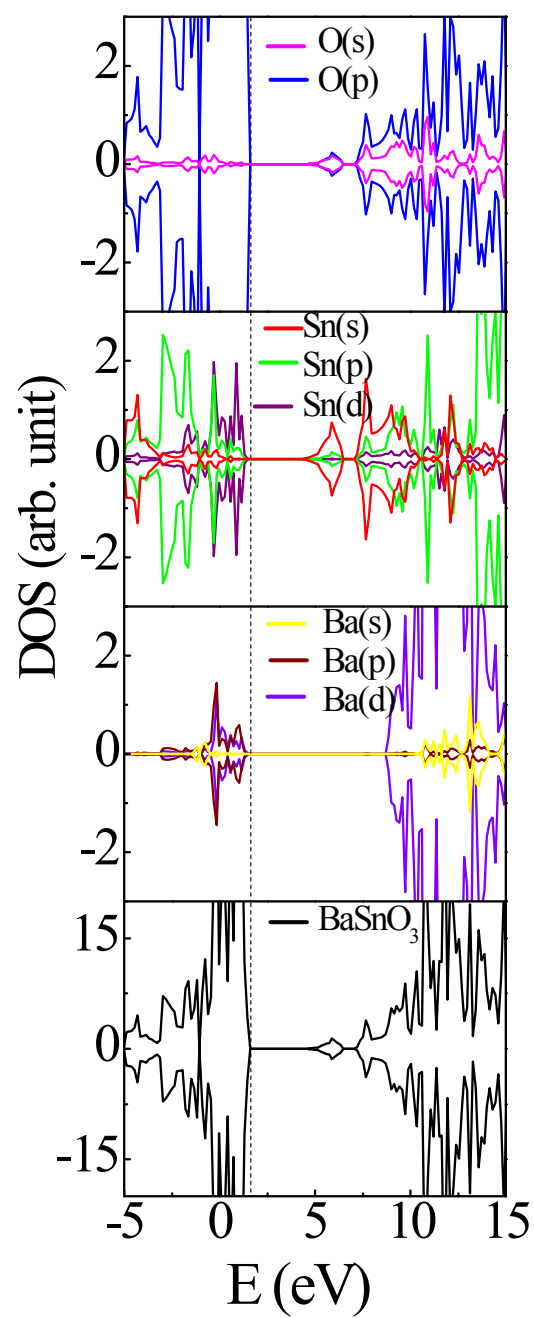


Figure S2: Density of states for BaSnO₃. Vertical dashed line indicates Fermi Level.

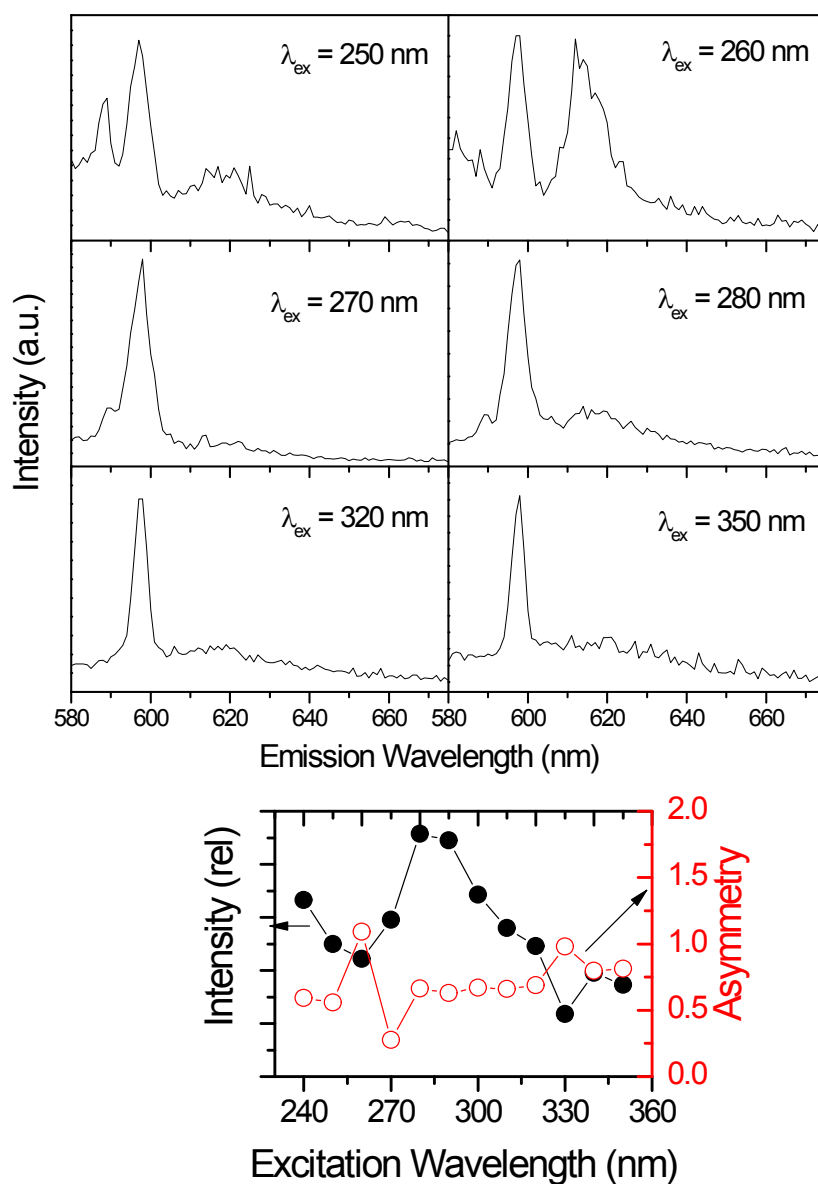


Figure S3. (Top) Emission map of 1.0% Eu^{3+} doped BaSnO_3 with different excitations. **(Bottom)** Variation in the emission intensity and asymmetry in the emission (EDT/MDT) with excitation wavelength.

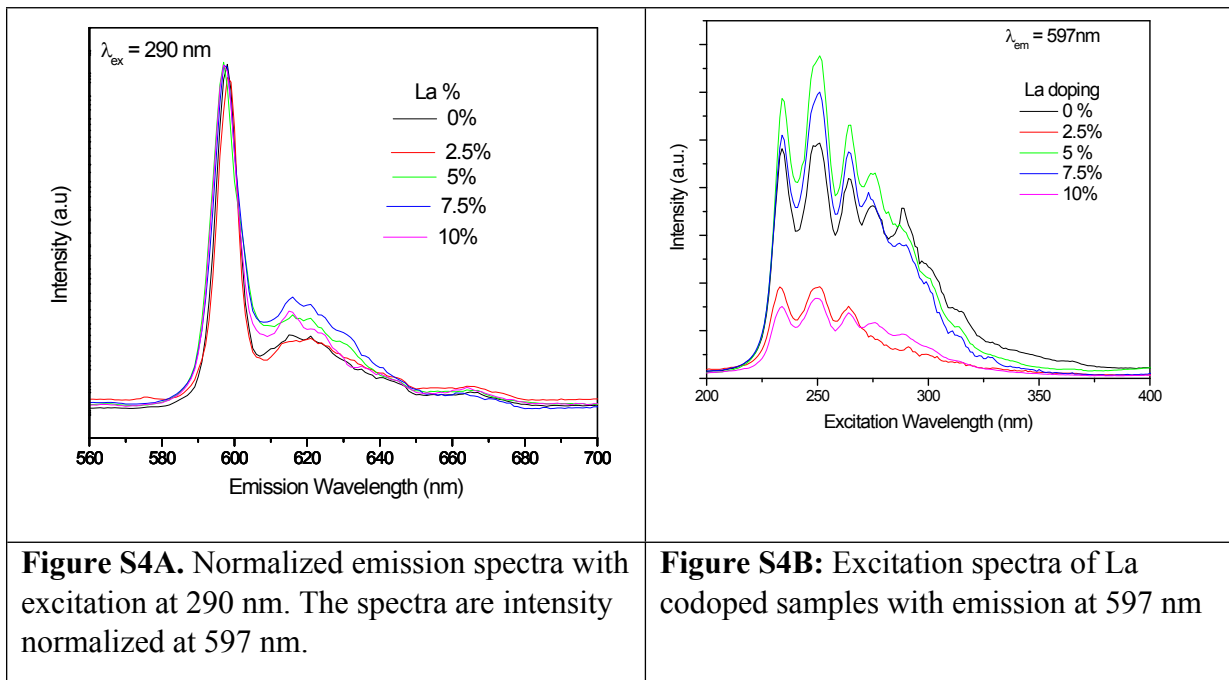


Figure S4A. Normalized emission spectra with excitation at 290 nm. The spectra are intensity normalized at 597 nm.

Figure S4B: Excitation spectra of La codoped samples with emission at 597 nm

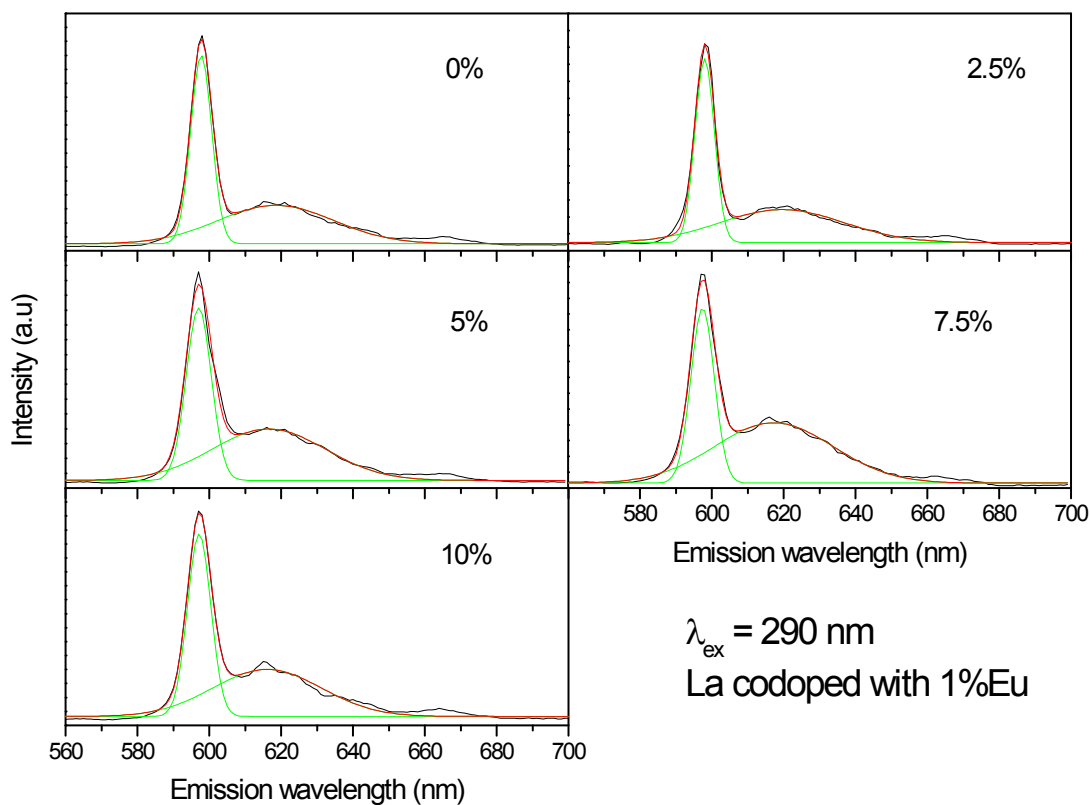


Figure S5: Deconvolution of the emission spectra in La codoped along with 1%Eu samples of BaSnO_3 for determining asymmetry in the emission.

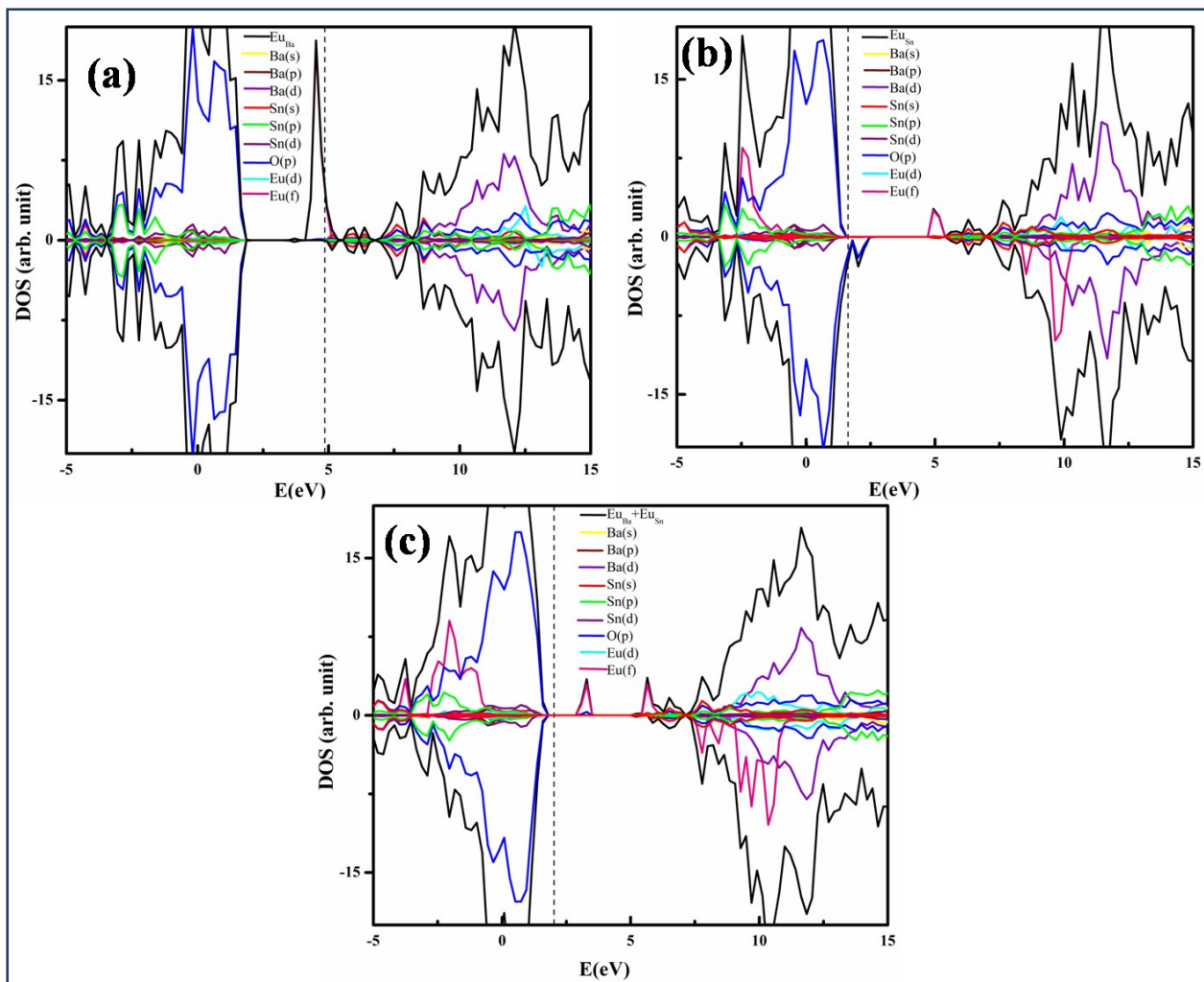


Figure S6: Density of states for BaSnO₃ containing Eu dopant at (A) Ba site (Eu_{Ba}), (B) Sn site (Eu_{Sn}) and (C) both Ba and Sn site ($\text{Eu}_{\text{Ba}} + \text{Eu}_{\text{Sn}}$). Vertical dashed line indicates Fermi Level.

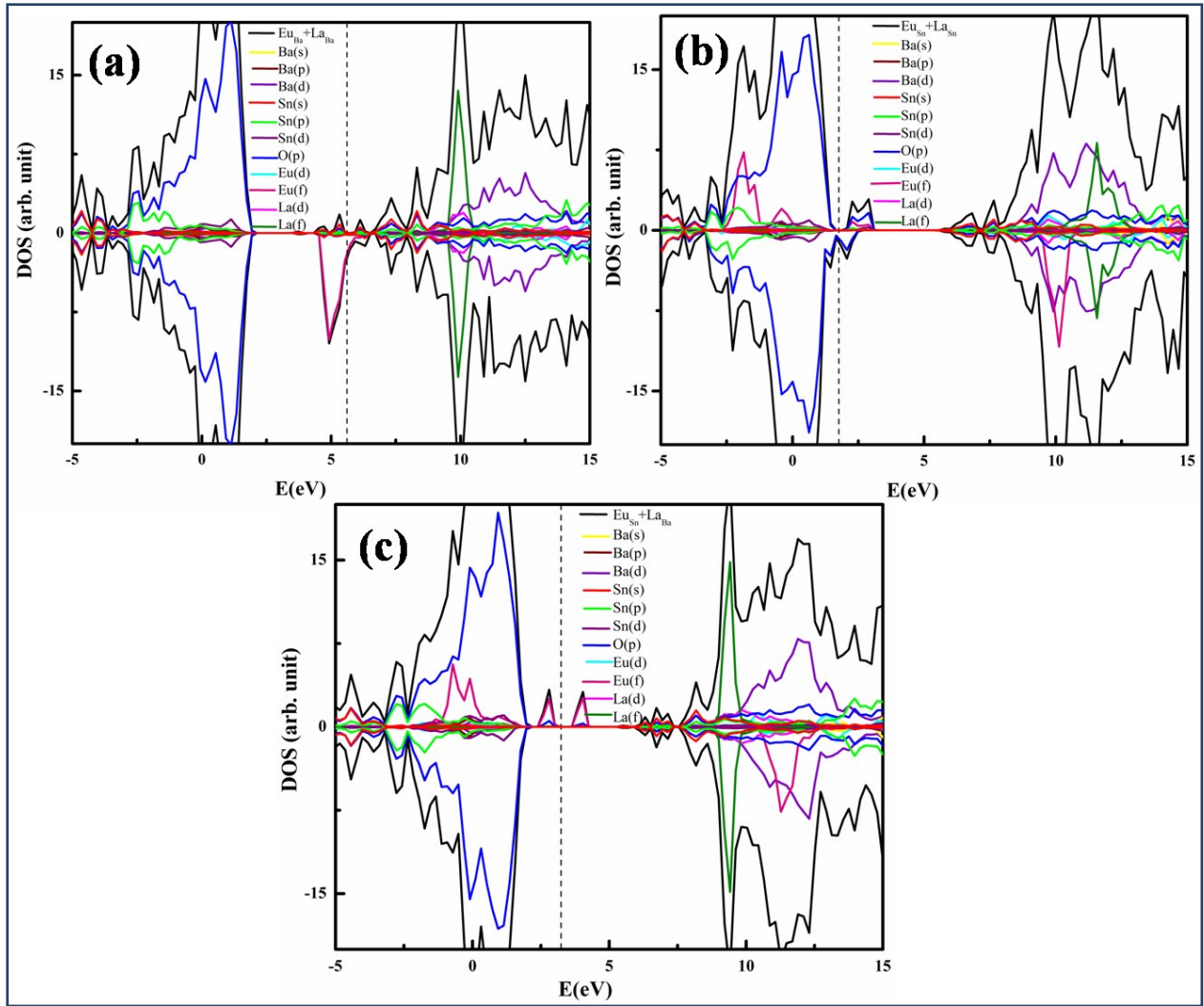


Figure S7: Density of states for BaSnO₃ containing Eu and La dopant at (a) Ba site (Eu_{Ba} + La_{Ba}), (B) Ba site (Eu_{Sn} + La_{Sn}) and (C) Eu and La dopant at Ba and Sn site respectively (Eu_{Sn} + La_{Ba}). Vertical dashed line indicates Fermi Level.

Table S1: PL and their origin in BaSnO₃ as reported by different groups

BaSnO ₃	Luminescence Peak	Origin	Remark
BaSnO ₃ microrod synthesized by co-precipitation[20]	Vey broad green luminescence	Inherent property of perovskite crystal family ABO ₃	Literature based explanation of peak
Sol-gel synthesized BaSnO ₃ [21]	Multiple weak peaks in visible reason and intense NIR peak	OVs for visible peaks and creation of sin centre near VB to NIR	No evidence and the explanation was referenced based
BaSnO ₃ thin films [22]	Peaks at 452 nm, 480 nm and 580 nm	Transfer of charge in the visible region between Sn ²⁺ and O ²⁻	No experimental or theoretical evidence

		levels	
BaSnO ₃ epitaxial film [23]	broad emission peak centered at 905 nm	Intrinsic defect	Interpretation is based on literature
Solid state synthesized BaSnO ₃ [24]	broad band centered at 905 nm (1.4 eV)	recombination of a photogenerated valence-band hole and an occupied donor level	Neither experimental nor theoretical evidence for the same
BaSnO ₃ nanopowder [25]	Blue and green emission	Electronic transition involving Ba ²⁺ and Sn ⁴⁺	Very unlikely
Microcrystalline BaSnO ₃ (This work)	Violet, Blue and Green emission	Oxygen vacancies	Based on DFT and PALS

Refernces:

- (1) Rodríguez-Carvajal J. JFULLPROF: a program for Rietveld, profile matching and integrated intensity refinements for X-ray and neutron data. Version. CEA-Saclay, France: Laboratoire Leon Brillouin; 2000.
- (2) E.H. Mountstevens, J.P. Attfield, S.A.T. Redfern, Cation-size control of structural phase transitions in tin perovskites, *J. Phys.: Condens. Matter* 15, 8315 (2003).
- (3) P. Kirkegaard, J.V. Olsen, M.M. Eldrup, and N.J. Pedersen, PALSfit: A computer program for analyzing positron lifetime spectra, Risø National Laboratory for Sustainable Energy, Technical University of Denmark, Roskilde, Denmark, **2009**, Risoe-R, No. 1652(EN).
- (4) Kresse, G.; Joubert, D. From Ultra soft Pseudo potentials to the Projector Augmented-Wave Method. *Phys. Rev. B: Condens. Matter Mater. Phys.* **1999**, *59*, 1758.
- (5) Blöchl, P. E. Projector Augmented-Wave Method. *Phys. Rev. B: Condens. Matter Mater. Phys.* **1994**, *50*, 17953.
- (6) Perdew, J. P.; Chevary, J. A.; Vosko, S. H.; Jackson, K. A.; Pederson, M. R.; Singh, D. J.; Fiolhais, C. Atoms, Molecules, Solids, and Surfaces: Applications of the Generalized Gradient Approximation for Exchange and Correlation. *Phys. Rev. B: Condens. Matter Mater. Phys.* **1992**, *46*, 6671.
- (7) Perdew, J. P.; Burke, K.; Ernzerhof, M. Generalized Gradient Approximation Made Simple. *Phys. Rev. Lett.* **1996**, *77*, 3865–3868.
- (8) Monkhorst, H. J.; Pack, J. D. Special Points for Brillouin-Zone Integrations. *Phys. Rev. B* **1976**, *13*, 5188.
- (9) Perdew, J. P.; Ernzerhof, M.; Burke, K. Rationale for Mixing Exact Exchange with Density Functional Approximations. *J. Chem. Phys.* **1996**, *105*, 9982-9985.
- (10) Adamo, C.; Barone, V. Toward Reliable Density Functional Methods without Adjustable Parameters: The PBE0 Model. *J. Chem. Phys.* 1999, *110*, 6158–6170.
- (11) V. Louis-Achille, L. De Windt, M. Defranceschi, Local density calculation of structural and electronic properties for Ca₁₀(PO₄)₆F₂, *Comput. Sci. Mater.* 10 (1998) 346.
- (12) M. Alatalo, B. Barbiellini, M. Hakala, H. Kauppinen, T. Korhonen, M. J. Puska, K. Saarinen, P. Hautojärvi and R. M. Nieminen, Theoretical and experimental study of positron annihilation with core electrons in solids, *Phys. Rev. B: Condens. Matter Mater. Phys.*, 1996, *54*, 2397.
- (13) H. D. Megaw, Crystal structure of double oxides of the perovskite type in *Proceedings of the Physical Society, London*, 1946, *58*, 133-152.

- (14) M. J. Puska and R. M. Nieminen, Defect spectroscopy with positrons: a general calculational method, *J. Phys. F: Met. Phys.*, 1983, 13, 333–346
- (15) B. Barbiellini, M. J. Puska, T. Torsti and R. M. Nieminen, Gradient correction for positron states in solids, *Phys. Rev. B: Condens. Matter Mater. Phys.*, 1995, 51, 7341
- (16) S. Basu, C. Nayak, A. Yadav, A. Agrawal, A. Poswal, D. Bhattacharyya, S. Jha, N. Sahoo, A comprehensive facility for EXAFS measurements at the INDUS-2 synchrotron source at RRCAT, Indore, India, *Journal of Physics: Conference Series*, IOP Publishing, 2014, pp. 012032.
- (17) Poswal, A. Agrawal, A. Yadav, C. Nayak, S. Basu, S. Kane, C. Garg, D. Bhattacharyya, S. Jha, N. Sahoo, Commissioning and first results of scanning type EXAFS beamline (BL-09) at INDUS-2 synchrotron source, *AIP Conference Proceedings*, American Institute of Physics, 2014, pp. 649-651.
- (18) *X-Ray Absorption: Principles, Applications, Techniques of EXAFS, SEXAFS and XANES*, edited by D.C. Konigsberger and R. Prince (Wiley, New York, 1988).
- (19) M. Newville, B. Ravel, D. Haskel, J.J. Rehr, E.A. Stern and Y. Yacoby, *Physica B* **154** (1995) 208.
- (20) S. Sharma, S. Chhoker, Efficient light harvesting using simple porphyrin-oxide perovskite system, *Scientific Reports* 10 (2020) 14121
- (21) S.M. Yakout, H.A. Mousa, H.T. Handal, W. Sharmoukh, Role of non-magnetic dopants on the room temperature ferromagnetism and optical properties of BaSnO₃ perovskite, *Journal of Solid State Chemistry* 281 (2020) 121028
- (22) J. John, S. Suresh, S.R. Chalana, V.P. Mahadevan Pillai, Effect of substrate temperature, laser energy and post-deposition annealing on the structural, morphological and optical properties of laser-ablated perovskite BaSnO₃ films, *Applied Physics A* 125 (2019) 743.
- (23) H. Takashima, Y. Inaguma, Near-infrared luminescence in perovskite BaSnO₃ epitaxial films, *Applied Physics Letters* 111 (2017) 091903.
- (24) H. Mizoguchi, P.M. Woodward, C.-H. Park, D.A. Keszler, Strong Near-Infrared Luminescence in BaSnO₃, *Journal of the American Chemical Society* 126 (2004) 9796-9800.
- (25) A.S. Deepa, S. Vidya, P.C. Manu, S. Solomon, A. John, J.K. Thomas, Structural and optical characterization of BaSnO₃ nanopowder synthesized through a novel combustion technique, *Journal of Alloys and Compounds* 509 (2011) 1830-1835